

Climate Change and Equestrian Empires in the Eastern Steppes: New Insights from a High-resolution Lake Core in Central Mongolia

Julian Struck (✉ julian.struck@uni-jena.de)

Institute of Geography, Physical Geography, Friedrich Schiller University Jena, Jena

Marcel Bliedtner

Institute of Geography, Physical Geography, Friedrich Schiller University Jena, Jena

Paul Strobel

Institute of Geography, Physical Geography, Friedrich Schiller University Jena, Jena

William Timothy Trear Taylor

University of Colorado-Boulder Museum of Natural History, Boulder, CO

Sophie Biskop

Institute of Geography, Geoinformatics, Friedrich Schiller University Jena, Jena

Birgit Plessen

Section Climate Dynamics and Landscape Evolution, GFZ German Research Centre for Geosciences, Potsdam

Björn Klaes

Department of Geology, University of Trier, Trier

Lucas Bittner

Institute of Geography/ Physical Geography with focus on paleoenvironmental research, Technische Universität Dresden, Dresden

Bayarsaikhan Jamsranjav

Max Planck Institute for the Science of Human History, Department of Archaeology, Jena

Gary Salazar

Department of Chemistry, Biochemistry and Pharmaceutical Sciences and Oeschger Centre for Climate Change Research, University of Bern, Bern

Sönke Szidat

Department of Chemistry, Biochemistry and Pharmaceutical Sciences and Oeschger Centre for Climate Change Research, University of Bern, Bern

Alexander Brenning

Institute of Geography, Geoinformatics, Friedrich Schiller University Jena, Jena

Enkhtuya Bazarradnaa

Institute of Plant and Agricultural Sciences, School of Agroecology and Business, Mongolian University of Life Sciences, Darkhan

Bruno Glaser

Institute of Agricultural and Nutritional Sciences, Soil Biogeochemistry, Martin-Luther University Halle-Wittenberg, Halle (Saale)

Michael Zech

Institute of Geography/ Physical Geography with focus on paleoenvironmental research, Technische Universität Dresden, Dresden

Roland Zech

Institute of Geography, Physical Geography, Friedrich Schiller University Jena, Jena

Research Article

Keywords: Climate change, equestrian empires , high-resolution lake core, Central Mongolia

Posted Date: October 21st, 2021

DOI: <https://doi.org/10.21203/rs.3.rs-965381/v1>

License:   This work is licensed under a Creative Commons Attribution 4.0 International License.

[Read Full License](#)

Abstract

The repeated expansion of East Asian steppe cultures was a key driver of Eurasian history, forging new social, economic, and biological links across the continent. Climate has been suggested as important driver of these poorly understood cultural expansions, but paleo-climate records from the Mongolian Plateau often suffer from poor age control or ambiguous proxy interpretation. Here, we use a combination of geochemical analyses and comprehensive radiocarbon dating to establish the first robust and detailed record of paleo-hydrological conditions for Lake Telmen, Mongolia, covering the past ~4000 years. Our record shows that humid conditions coincided with solar minima, and hydrological modelling confirms the high sensitivity of the lake to paleo-climate changes. Careful comparisons with archaeological and historical records suggest that in the vast semi-arid grasslands of eastern Eurasia, solar minima led to reduced temperatures, less evaporation, and high biomass production, expanding the power base for pastoral economies and horse cavalry. Our findings suggest a crucial link between temperature dynamics in the Eastern Steppe and key social developments, such as the emergence of pastoral empires, and fuel concerns that global warming enhances water scarcity in the semi-arid regions of interior Eurasia.

1. Introduction

The rise of transcontinental, pastoral empires linking eastern and western Eurasia across the steppes had a tremendous transformative effect on human societies, facilitating the spread of people, goods, and ideas – as well as organisms like domestic animals, plants, and catastrophic disease¹⁻⁴. The Mongolian steppe was first occupied by pastoral people ca. 3000 BCE, when early herders appear to have migrated to the region from western Asia⁵⁻⁷. Around 1200 BCE, domestic horses were used first for transport by mobile herders of the Deer Stone-Khirgsuur complex (DSK) and other Bronze Age culture groups⁸⁻¹¹. The emergence of horse culture changed mobility of the steppe cultures, leading to the rise of important nomadic polities like the Xiongnu (ca. 200 BCE – 100 CE) and the Great Mongol Empire, who rose to global dominance under Genghis Khan in the early 13th century CE^{10,12}. For these pastoral empires, extensive and productive grasslands provide the engine for both economic and political power^{13,14}. Yet, particularly in the dry and harsh steppes of eastern Eurasia, minor climate variations can have large impacts on the water balance, biomass production, and ecosystem carrying capacity¹⁵⁻¹⁷. The close coupling between precipitation and temperature regimes and domestic animal productivity has inspired hypotheses that climate changes may have played an important role for network formation and human history in Central Asia¹⁷. While social-economic changes such as the emergence of social inequality in pastoral societies can be well inferred from historical and archaeological records^{11,17,18}, potential climatic controls can only be assessed by high-resolution paleoclimate records, which are currently rare for the Late Holocene in Mongolia.

Paleoclimate information derived largely from lake sediments¹⁹⁻²⁶ and tree-rings^{13,27-29}, suggest a possible link between the onset of wetter conditions and social integration among Mongolian

pastoralists. For northern and Central Mongolia, many records indicate a shift to humid conditions with the onset of the Late Holocene. Increasing moisture availability around 1000 BCE^{19,30} was suggested to favor the expansion of nomadic tribes³¹. For the past ~1500 years high resolution tree-ring records show short-term temperature fluctuations^{27–29,32}, that can be attributed to volcanic forcing^{33,34}. Pederson et al.¹³ identified more persistent droughts during the Medieval Climate Anomaly (MCA; 850 - 1300 CE), followed by warmer and more humid conditions between 1211 and 1225 CE, which could have favored the expansion of the Mongol Empire.

Despite these tantalizing links between climate changes and pastoral dynamics, the paleoclimatic and -environmental records for Mongolia suffer from poor temporal resolution, age uncertainties, and/or ambiguous proxy interpretation. Oftentimes, chronological frameworks designed for geological research questions (with wide error ranges) are applied to archaeological timescales, meaning that the same dataset can be used to draw widely differing conclusions³⁵. Anthropogenic impacts related to herding have also drastically impacted Mongolia's landscape – meaning that pollen and any other biological data, for example, might be affected by human land-use since 1200 or even 3000 BCE^{8,30}. In order to provide a more convincing link between climate and human history, more robust and well-dated high-resolution paleo-climate records are needed. Here, we report a single well-dated paleohydrological record that spans the whole timeline of Mongolian pastoral history and prehistory from the late Bronze Age, allowing the first proper opportunity to test for a causal link between climate dynamics and pastoral empires in the eastern Steppe.

In this study, we investigated a 161 cm long sediment core from Lake Telmen, an endorheic lake in Zavkhan province in semi-arid central Mongolia, along the western edge of the Khangai Mountains (Supplementary Fig. 1). We applied radiocarbon dating on bulk TOC and molecular markers to establish a robust chronology, and we combined compound-specific $\delta^2\text{H}$ and $\delta^{13}\text{C}$ on individual *n*-alkanes, bulk $\delta^{13}\text{C}$ and $\delta^{18}\text{O}$ on carbonates, with elemental and inorganic geochemical and sedimentological analyses to establish a detailed paleo-environmental record and to precisely constrain the regional hydrological history. Moreover, the lake's sensitivity to changes in temperature and precipitation was evaluated by a hydrological water balance model, which enables an identification of relevant forcings.

2. Results

2.1 Sediment core chronology

The lowermost and oldest radiocarbon age from our sediment core is 2300 ± 170 BCE, while a present-day water plant reveals a hard-water effect (Δ_{HW}) of 190 ± 83 years (Supplementary Tab. 1). We established an age-depth model (ADM) using seven Δ_{HW} -corrected bulk ^{14}C ages and two compound-class *n*-alkane ^{14}C ages (Supplementary Fig. 2). The ^{14}C chronology is stratigraphically very consistent (Supplementary Fig. 2, Supplementary section S2). We further refined the ADM using nine tie points that we identified by comparison with total solar irradiance (TSI)³⁶ (Fig. 1, Supplementary Fig. 3, see "Method

section"). The (Δ_{HW} -corrected) ^{14}C ages overlap with the 95% confidence interval of the tie-point ADM, and the median ages of both ADMs differ by no more than 246 years.

2.2 Sedimentological and geochemical analyses

Our sediment core is finely laminated, mainly consists of silty siliciclastic components ($\geq 66\%$) and is characterized by high amounts of total organic carbon (TOC: 5.4 – 12.3%) and carbonates (total inorganic carbon, TIC: 3.2 – 6.3%) (Supplementary Fig. 4). The carbonates are dominated by monohydrocalcite (MHC), calcite and minor dolomite (Supplementary Figs. 4, 6). Element analyses show significant correlations ($\alpha = 0.05$) for Al, Fe, and K, for Mg and Na, and for Ca and Sr, respectively (Supplementary Tab. 2). The first principal component (PC1) describes 53.3% of the variance and shows strong positive loadings for Al, Fe, and K. PC2 describes 36.1% of the variance and has strong positive loadings for Na and Mg, and strong negative loadings for Ca (Supplementary Fig. 5). PC1 can be interpreted to reflect allochthonous input related to weathering and erosion processes in the catchment³⁷, whereas PC2 characterizes the autochthonous production (Supplementary Fig. 5). With regard to our geochemical data, the most relevant paleo-hydrological information is inferred from the Ca/Al ratio, which ranges from 4.7 to 23. Wide ratios indicate enhanced autochthonous production and carbonate precipitation during probably dry and warm periods around 1500 BCE and again around 1000 CE (Fig. 2a). Narrow ratios indicate more allochthonous input in between 1200 BCE and 700 CE, as well as after ~1300 CE, which can be interpreted to document humid conditions with elevated runoff.

2.3 Isotope analyses, evaporation index (E_I), and paleo-hydrology

n-Alkanes were present in all samples in sufficient amounts for compound-specific isotope analyses (Supplementary Fig. 7). A differentiation of allochthonous and autochthonous compounds can be made on the basis of *n*-alkane chain lengths. *n*-C₃₁-Alkanes are predominantly synthesized by higher terrestrial plants and are of allochthonous origin^{37,38}. Therefore, our $\delta^2\text{H}_{n\text{-C}_{31}}$ record mainly reflects changes in the isotopic signature of precipitation³⁹. Changes were minor over the past 4000 years, since $\delta^2\text{H}_{n\text{-C}_{31}}$ is relatively constant, ranging from -219 ± 2.0 to $-193 \pm 2.1\text{‰}$ (Fig. 2b). *n*-C₂₃-Alkanes, on the other hand, are predominantly synthesized by aquatic plants³⁷. Thus, our $\delta^2\text{H}_{n\text{-C}_{23}}$ record reflects the isotopic signature of lake water and its evaporative ^2H enrichment⁴⁰⁻⁴³. $\delta^2\text{H}_{n\text{-C}_{23}}$ ranges widely from -180 ± 3.5 to $-139 \pm 2.7\text{‰}$ and indicates lake water ^2H enrichment in distinct periods, particularly before 1500 BCE (Fig. 2c).

Since, the carbonates in Lake Telmen are also predominantly of autochthonous origin, $\delta^{18}\text{O}_{\text{carb}}$ – which ranges from -2.5 to 0.5‰ – also reflects the isotopic signature and evaporative ^{18}O enrichment of lake water⁴⁴⁻⁴⁶. Like $\delta^2\text{H}_{n\text{-C}_{23}}$ the $\delta^{18}\text{O}_{\text{carb}}$ record shows maximum enrichment before 1500 BCE (Fig. 2d). Significant co-variation between $\delta^{18}\text{O}_{\text{carb}}$ and $\delta^{13}\text{C}_{\text{carb}}$ ($r = 0.61$, $p = 1.06e^{-17}$) reflects evaporation under equilibrium conditions of dissolved and atmospheric CO_2 and indicates the paleo-hydrological sensitivity

of both isotopes^{44–46}. $\delta^{13}\text{C}_{\text{carb}}$ ranges from 1.3 to 3.1‰ with maximum values again before 1500 BCE, but also relatively high values around 1000 CE (Fig. 2e).

$\delta^2\text{H}_{n\text{-C23}}$, $\delta^{18}\text{O}_{\text{carb}}$, and $\delta^{13}\text{C}_{\text{carb}}$ show similar down-core trends and primarily reflect the evaporative enrichment of lake water. We therefore combined all three proxies into a normalized Evaporation Index (E_I ; Fig. 2f, Supplementary Fig. 8). Positive E_I values document enhanced evaporative lake water enrichment under dry conditions, which also leads to reduced moisture effectively available for the ecosystems at our study site. We refer to this as “dry” in the following. By contrast, negative E_I values document reduced evaporative enrichment due to colder and/or more humid conditions, which leads to increased effective moisture in this ecosystem (referred to as “humid”).

As illustrated in Figure 3f, the E_I reveals dry conditions for the early Late Holocene until ca. 1200 BCE, followed by a long-lasting humid period from 1200 BCE to 700 CE. From 700 to 1300 CE, regional climate conditions became drier again, temporally coinciding with the MCA. With the onset of the Little Ice Age (LIA) around 1300 CE, regional climate tended to be more humid. This dry-humid-dry-humid pattern perfectly agrees with the Ca/Al ratio, corroborating the interpretation and robustness of the various proxies.

Our results show a transition from dry to humid conditions around 1200 BCE, associated with directional socio-economic changes in Mongolian pastoralist cultures^{8,9}. Wetter conditions are associated with the onset of sedimentation in the western shallow lake basin previously dated to 1300 BCE²² and a prominent lake level rise of 9.4 m indirectly dated to ca. 0 CE²². Another lake high-stand is recorded by a prominent +4.8 m shoreline terrace, which has been directly dated to between 600 and 700 CE²² and very likely points to a humid phase shortly before the onset of the drier MCA.

3. Discussion

3.1 External forcing on the regional climate

Our results suggest that these long-term humidity trends are driven by changes in solar insolation (Fig. 3a). On the one hand, reduced summer insolation leads to a weakening of the monsoon system and thus to less precipitation in the areas affected by the monsoonal system and higher precipitation in the adjacent northern regions (sometimes referred to “Arid Central Asia”) including Mongolia⁴⁷ (Supplementary Fig. 1). This effect can be explained with weak subsidence and more prominent convection. On the other hand, a long-term reduced summer insolation ($\sim 6 \text{ Wm}^{-2}$ from the Mid- to the Late Holocene, Fig. 3a) will inevitably lead to lower temperatures, reduced evaporation and more effective ecosystem moisture (Supplementary section S7).

However, superimposed on this long-term trend we find a strong resemblance of our E_I record with short-term fluctuations of the high-resolution TSI record (Fig. 3b, e). The solar minima at ~ 800 BCE, 400 BCE,

as well as ~700 CE and after 1300 CE all coincide with prominent minima displayed by our E_i record. We interpret this as strong empirical evidence for solar forcing being the most important factor influencing the local hydrological conditions at our site.

TSI varies by about 1 Wm^{-2} , which modifies the radiative forcing at the Earth's surface and the mean global temperature by $\sim 0.17 \text{ Wm}^{-2}$ and $\sim 0.07^\circ\text{C}$, respectively⁴⁸. Lean⁴⁹ suggested a higher sensitivity for the mid-latitudes and regional temperature modifications of up to 2°C . A temperature decrease at this magnitude should entail a significant decrease of evaporation, which directly affects the regional moisture balance (see section "Hydrological modelling" below). In addition, reduced TSI during solar minima favored northern hemispheric cooling, which strengthened latitudinal temperature gradients and the Westerly jet streams^{48,50,51}. Then, the North Atlantic Oscillation (NAO) tends to be in a distinct negative mode (Fig. 3c), which forces the Westerly jets to the South, advecting more moisture to "Arid Central Asia", and thus, our research site^{21,51} (Supplementary Fig. 1). In contrast, higher TSI leads to reduced latitudinal temperature gradients, which coincides with a distinct positive NAO mode (Fig. 3b, c) as well as a northward shift of the Westerly jets^{21,51}, which favors dry conditions at Lake Telmen.

3.2 Hydrological modelling

To evaluate how temperature and precipitation changes related to solar forcing could have impacted the water balance of Lake Telmen, we set up a hydrological model (Supplementary Tab. 3). The model-simulated long-term average water balance of Lake Telmen indicates a state close to equilibrium, which coincides well with the relatively stable average lake extent of Lake Telmen over the past decades⁵². Several sensitivity tests show that the water balance is highly sensitive to changes in temperature and precipitation (Supplementary Tab. 4). A 1°C decrease in air temperature (and lake surface temperature, respectively), for example, reduces lake evaporation by already 5% or 8%, respectively.

During the lake high-stand of +4.8 m above present (600 - 700 CE)²², the lake area was 13% larger than today (Supplementary Fig. 1). To maintain the corresponding water balance state close to equilibrium, air temperature would need to be 0.35°C lower, or precipitation would need to be 2.5% higher ($\sim 12 \text{ mm a}^{-1}$) compared to present-day conditions. Considering the joint effect of air and water temperatures, a decrease of only 0.15°C would already be sufficient. This highlights that even small temperature changes related to solar forcing (Fig. 3b) could explain the observed hydrological changes and lake level fluctuations. The +4.8 m lake high-stand could therefore be explained by the solar minimum at ~700 CE, while age uncertainties in this part of the core section do not rule out a potential correlation of this particular lake high-stand with the Late Antique Little Ice Age (LALIA; 536- 660 CE)³², which marks the onset of prominent temperature anomalies within the common era⁵³. Major volcanic eruptions may have reduced temperatures by up to 2.5°C at 536 CE and 543 CE^{33,34}. Our hydrological model suggests that such a strong, short-term temperature decline would maintain a water-balance state close to equilibrium – even if precipitation decreased by 18% relative to present-day conditions. All this confirms that Lake Telmen and the hydrological water balance at the study site are extremely sensitive to solar forcing and even small temperature changes.

3.3 Climate impact on human history in Mongolia

Sustained humid conditions likely enabled the expansion of fertile grasslands and thus, increased ecosystem carrying capacity^{14,17,54} – allowing to raise larger numbers of livestock and horses for both meat and dairy production^{9,11}. Particularly in the dry and seasonal steppe environment, domestic livestock herds experience “economies of scale” – wherein smaller herds are more vulnerable to loss from disease, predation, or weather, and larger herds are more resilient⁵⁵. With productive areas distributed unequally across the landscape, and some herders inevitably subject to disaster and loss, periods of environmental productivity appear to encourage the formation of larger steppe social networks¹⁷. As the key engine of preindustrial transport and warfare in Eurasia, horses directly impacted the military and transport capacity of steppe societies, while long military campaigns also often required grazing areas for other livestock⁵⁶. Together, these and other factors likely helped create an uncommonly close causal link between environmental dynamics and sociopolitical developments in the Mongolian grasslands.

The onset of humid conditions at 1200 BCE (Figs. 2, 3) coincides with drastic social changes across Central Mongolia, including the first emergence of horse culture and evidence for widespread social integration across the eastern steppe. In contrast to earlier pastoralists, who were apparently constrained largely to mountain margins, DSK and other late Bronze Age herders made use of open grassland and desert regions⁸. At some sites, hundreds or even thousands of horse burials testify to the expanded ecological and social significance of horses⁵⁷. The epicenter of this dramatic emergence of horse culture appears to have been Central Mongolia, with large funerary and monument complexes emerging in the Central Mongolian Khangai Mountain Range (including Zavkhan province)^{58–60}. Our results suggest that the expansion of the region’s first culture, which spread as far as Trans Baikal, Tuva, Kazakhstan, Xinjiang, and China, was supported by wet conditions driven by a solar minimum.

While the NAO weakening during the grand solar minimum is associated with a general climate and environmental crisis⁵¹, triggering human migrations and the collapse of cultures in large parts of northern Europe^{61,62}, we find the opposite causal link in Mongolia – between increased effective ecosystem moisture and positive socio-environmental impacts due to enhanced biomass production and an expansion of fertile grasslands^{15,16,63}. During the grand solar minimum from 800 to 600 BCE (Fig. 3d, l.)⁶⁴ in key social changes, and the emergence of the first integrated pastoral empires took place during a prolonged period of humid conditions, as indicated by our E_i . As the DSK culture waned, Mongolia witnessed an expansion of the Slab Burial culture, whose sites also yield the first direct evidence of riding tack⁶⁵, royal equestrian burials and the earliest evidence for horsemanship appear in the archaeological record at Arzhan, in Tuva, and early mounted Scythian groups spread westward out of interior Asia⁶⁶.

From this first expansion of horse culture, a prolonged period of humid conditions in central Mongolia supported the convergence of Mongolia’s first united pastoral polities. The Xiongnu Empire thrived particularly between 200 BCE and 100 CE (Fig. 3f)^{10,67,68}, when climate conditions were also predominantly humid. Extensive fertile grasslands favored pastoralism, while this period also saw the

adoption of agriculture, the establishment of village-like settlements, increased gene flow with East and Central Asia, and extensive trade relations were established as far as the Mediterranean^{7,10,12,68}. Complemented by new military and organizational techniques, climatic and environmental conditions favorable for animal pastoralism enabled the Xiongnu to form a large and powerful politically structured empire^{6,8,12,31,67}.

This prolonged period of favorable climate-human interaction seems to have persisted across the early first millennium CE. This record shows that humid conditions were no guarantee of persistent political stability, as some important polities rose and fell in the Mongolian steppe. However, after the Xiongnu state failed ca. 100 CE, both the Rouran Khaganate (ca. 400 CE) and the first Turkic Khaganate (ca. 550 CE) formed during periods of favorable grassland conditions in Central Mongolia¹⁰. This run ended with the onset of the LALIA around 600 CE (Fig. 3b-f).

Just as solar minima appear to have been crucial to the first formation of pastoral empires, solar maxima may have had a disruptive effect on social integration in ancient Mongolia. Very harsh and long winters seem to have caused high livestock mortality, an increase in warfare activity, famines, and cultural re-organization during the LALIA^{6,10,27,28,32}. Based on our record, dry climate conditions prevailed during the MCA in Central Mongolia, and conditions remained unfavorable until the end of the MCA around 1300 CE. Under these conditions, failing grassland biomass may have undercut the economic and social power base of the first Turkic Khaganate, and contributed to its disintegration in ca. 603 CE⁶⁹. During subsequent centuries, Mongolia cycled through a comparatively tumultuous period of political instability, with brief periods of steppe integration like the Second Turkic (ca. 680-740 CE) and Uyghur (ca. 750-850 CE) Khanates, interspersed with periods of domination by external powers like the Tang and Khitan states^{10,70}.

Finally, our record supports previous arguments that moisture balance also played an important role in the emergence and success of the largest pastoral empire, the Great Mongol Empire of Genghis and Khubilai Khan. Our E_f shows a shift to humid conditions since 1100 CE and a positive effective moisture balance at the MCA-LIA transition around 1300 CE (Fig. 3e). This likely favored the union of nomadic tribes under Genghis Khan and the formation of the Mongol Empire, which began during the early 13th century and reached its greatest spatial extent during the late 13th through the mid-14th century (Fig. 3f)^{13,14,54}.

We conclude that solar forcing played an important role in controlling regional climate at Lake Telmen over the past 4000 years. We have shown that even small changes in temperature and precipitation have a huge impact on the effective ecosystem moisture balance and thus, biomass production and the expansion of fertile grasslands. This apparent causal link between favorable climate conditions and positive socio-environmental impacts for herding cultures in the Mongolian steppe likely had tremendous impact on the broader trajectory of human history in Eurasia, as the cyclical emergence of pastoral

cultural networks and empires helped to forge some of the first pan Eurasian trade networks, spreading goods, plants, and animals, people, ideas, and even catastrophic pandemic disease¹⁻⁴.

While these moisture fluctuations seem to have exerted an important impact on the rise and fall of Mongolian steppe cultures over the past 4000 years, in light of the paleoclimate record we expect that the near-future consequences of global warming will put the ecosystems and livelihood of the pastoral population in Central Asia at great risk. Mongolia is already experiencing a 2°C temperature increase since 1963⁷¹, and will likely exceed TSI-induced temperature fluctuations in the near-future. Previous studies have shown a rapid loss of lakes⁵², melting mountain ice⁷², persistent soil moisture deficits^{73,74}, and an increased frequency of droughts^{73,75,76} and heavy rainstorms^{15,77,78}. Increased rainfall may not counteract the impact of rising temperatures. Instead, rainfall may exacerbate ongoing land degradation as these short-term heavy rainstorms exceed the soil's infiltration capacity and cause surface runoff, soil erosion, and even floods^{77,78}. Although, modeling results show a low probability that future drought intensities will exceed those of the last two millennia⁷⁶, present-day climate changes already cause enhanced socio-environmental consequences^{15,75,77}, and it is uncertain whether and how modern pastoralists will adapt to the future climate.

Methods

Coring:

A 161 cm long sediment core (TL-2017/1-1) was retrieved from 22 m water depth in 2017 (48°48'37.98" N, 97°20'43.9188" E), using an UWITEC corer with hammer action (UWITEC, Mondsee, Austria).

Sedimentological and geochemical characteristics:

Detailed descriptions of determining the grain size distribution, elemental, and mineral composition are provided in the Supplementary Methods.

Sediment core chronology:

The chronology of the Lake Telmen sediment record consists of nine tie-points we identified by comparison of our evaporation index (E_i) with the TSI record of Steinhilber et al.³⁶. For each tie point, we used corresponding ages from the 22-year averaged TSI record: 1 = 1295 CE, 2 = 1141 CE, 3 = 1053 CE, 4 = 943 CE, 5 = 745 CE, 6 = 679 CE, 7 = 355 BCE, 8 = 795 BCE, 9 = 1389 BCE³⁶. A Bayesian age-depth model was calculated with the package rbacon 2.4.3 in R 4.0.2⁷⁹. All ages presented in this paper are calibrated and given as BCE (before common era) and CE (common era).

Bulk isotopic composition of carbonates ($\delta^{13}\text{C}_{\text{carb}}$, $\delta^{18}\text{O}_{\text{carb}}$):

157 samples (ground and sieved $<40\mu\text{m}$) were measured with an automated carbonate-extraction device (KIELIV), coupled to a MAT253 IRMS (Thermo Fischer Scientific, Bremen, Germany) at the Helmholtz Centre Potsdam (GFZ). Up to 0.2 mg were automatically dissolved with 103% H_3PO_4 at 70°C under vacuum and the isotopic composition were subsequently measured on the released and cryogenic purified CO_2 . The isotope ratios are given in delta notation against the Vienna Pee Dee Belemnite (VPDB) standard. Analytical precision was checked using replicate measurements of reference materials (NBS19, C1-internal standard), and yielded standard errors $<0.07\text{‰}$ for both, $\delta^{13}\text{C}_{\text{carb}}$, $\delta^{18}\text{O}_{\text{carb}}$.

n-Alkane extraction and compound-specific $\delta^2\text{H}_{n\text{-alkane}}$ measurements:

Total lipids of 120 sediment samples (0.4 – 4.5 g) were ultrasonically extracted using a mixture of dichloromethane and methanol (9:1, v/v) as a solvent, the procedure was repeated in three cycles of 15 min each³⁸. Total lipid extracts were separated by solid phase extraction using aminopropyl (Supelco; $45\mu\text{m}$) as stationary phase, *n*-alkanes were eluted with hexane and additionally purified over coupled silver-nitrate (AgNO_3) coated silica gel (Supelco, 60-200 mesh) and zeolite (Geokleen Ltd.) pipette columns. Analytical measurements were performed at Friedrich Schiller University Jena. *n*-Alkane identification and quantification were performed on an Agilent 7890B gas chromatograph (Agilent, Santa Clara, California, USA) equipped with an Agilent HP5MS column ($30\text{ m} \times 320\mu\text{m} \times 0.25\mu\text{m}$ film thickness) and a flame ionization detector (GC-FID). For identification and quantification, external *n*-alkane standards (*n*-alkane mix $n\text{-C}_{21}$ – $n\text{-C}_{40}$, Supelco) were measured with each sequence. *n*-Alkane concentrations are given in micrograms per gram ($\mu\text{g g}^{-1}$) dry weight and were calculated as the sum of $n\text{-C}_{23}$ to $n\text{-C}_{35}$.

$\delta^2\text{H}_{n\text{-alkane}}$ analyses were performed on an isoprime visION isotope ratio mass spectrometer (Elementar, Manchester, UK) coupled via a GC5 pyrolysis–combustion interface (Elementar, Manchester, UK) to an Agilent 7890B gas chromatograph equipped with an Agilent HP5GC column ($30\text{m} \times 320\mu\text{m} \times 0.25\mu\text{m}$ film thickness). The GC5 operated in pyrolysis mode (ChromeHD reactor) at 1050°C . Samples were injected in splitless mode and measured in triplicates. *n*-Alkane standards ($n\text{-C}_{27}$, $n\text{-C}_{29}$ and $n\text{-C}_{33}$) with known isotopic composition (Schimmelmann *n*-alkane standards, Indiana, USA) were measured as duplicates after every third triplicate. The standard deviation for the triplicate measurements was $<3.6\text{‰}$ for $\delta^2\text{H}_{n\text{-C}_{23}}$ and $<6.1\text{‰}$ for $\delta^2\text{H}_{n\text{-C}_{31}}$. However, the relatively high maximum standard deviation for $\delta^2\text{H}_{n\text{-C}_{31}}$ concerns only one sample triplicate and the standard deviation was $<2.7\text{‰}$ for the remaining $\delta^2\text{H}_{n\text{-C}_{31}}$ triplicates. The standard deviation of standard duplicates was $<4.3\text{‰}$ ($n = 124$). $\delta^2\text{H}_{n\text{-alkane}}$ measurements were drift and amount-corrected relative to the standards in each sequence. The H3+

correction factor was checked routinely after system tuning and was stable at 4.2 ± 0.63 ($n = 15$). The compound-specific isotopic composition is given in delta notation versus the Vienna Standard Mean Ocean Water (VSMOW).

The evaporation index (E_I):

The E_I is based on predominantly autochthonous stable isotope values ($\delta^{13}\text{C}_{\text{carb}}$, $\delta^{18}\text{O}_{\text{carb}}$, and $\delta^2\text{H}_{n\text{-C}23}$), which are sensitive to lake evaporation causing a distinct enrichment in ^{13}C , ^{18}O , and ^2H , respectively. Since multiple isotope fractionation processes on each isotope can alter the isotopic signatures differently, all isotope values were z-transformed for standardization. The three isotopes show a similar down-core trend in terms of relative enrichment and depletion, respectively, and the E_I was calculated as the average of the z-standardized values.

Water balance modelling, sensitivity analysis and model scenarios:

The hydrological model J2000g adapted and extended according to the specific characteristics of closed-lake basins on the Tibetan Plateau⁸⁰, was transferred to the Lake Telmen basin. A detailed description of the model components, model-parameter estimation and input data requirements are given in Biskop et al.⁸⁰. As meteorological input we used climate station data (1990-2020) from Tosontsengel and lake surface water temperature from the ARC Lake data set (v3.0)⁸¹. To better understand the sensitivity of lake response to climate variability, we explored the effects of changes in climate input variables on several hydrological model-output components (lake evaporation, actual evapotranspiration, runoff). Lake-level changes were estimated by using the stage volume curve derived from the digital bathymetry and elevation (SRTM) elevation. Considering the paleo-lake extension of Lake Telmen, the hydrological model built for present-day conditions was run through several scenarios of precipitation and temperature changes in order to gain more quantitative knowledge about climatic conditions needed to maintain high lake-level stands during the Late Holocene. We calculated the paleo-lake extension for the +4.8 m and +9.4 m terrace above the present-day lake level²² using the water-level area curve derived from digital elevation and bathymetric data (Supplementary Figure 1).

Applied statistics:

Pearson's correlation coefficients (r values) were calculated to identify correlations within the geochemical and stable isotope dataset. Significance of correlations were tested using a two-sided t-test ($\alpha = 0.05$). For autochthonous and allochthonous endmember identification, we further calculated a principal component analysis for the elements Al, Fe, K, Mg, Na, Sr, and Ca. The applied statistic was performed with the statistical software Origin (version Pro 2019b).

Declarations

Data availability

The dataset used for this study will be uploaded to PANGEA.

Acknowledgements

P. Strobel acknowledges the support by a fellowship from the state of Thuringia (Landesgraduierstipendium). G. Daut (Friedrich Schiller University Jena) is acknowledged for taking the sediment core in 2017 and for data discussion. T. Kasper (Friedrich Schiller University Jena) and T. Haberzettl (University of Greifswald) are acknowledged for support during core opening and sampling as well as data discussions. We greatly acknowledge M. Benesch (Martin Luther University Halle-Wittenberg) for compound-specific $\delta^{18}\text{O}$ measurements, S. Pinkerneil (GFZ Potsdam) for bulk carbonate $\delta^{18}\text{O}$ and $\delta^{13}\text{C}$ measurements. N. Ueberschaar (MS platform, Friedrich Schiller University Jena) and J.-F. Wagner (Trier University) are acknowledged for providing laboratory facilities. We want to further acknowledge H. Maennicke, T. Bromm, S. Polifka, M. Lerch (all Martin Luther University Halle-Wittenberg), M. Wagner, B. Enyedi, C. Spittler, F. Freitag, I. Paetz, and N. Blaubach (all Friedrich Schiller University Jena), and O. Baeza-Urrea (Trier University) for laboratory support. We thank our logistic partners in Mongolia and all participants of the fieldtrip in 2017.

Conflict of interest

The authors declare no competing interest.

References

1. Spyrou, M. A. *et al.* Phylogeography of the second plague pandemic revealed through analysis of historical *Yersinia pestis* genomes. *Nature communications* **10**, 4470; 10.1038/s41467-019-12154-0 (2019).
2. Jiang, L., Guli, J., Bao, A., Guo, H. & Ndayisaba, F. Vegetation dynamics and responses to climate change and human activities in Central Asia. *The Science of the total environment*, **599-600**, 967–980 <https://doi.org/10.1016/j.scitotenv.2017.05.012> (2017).
3. Rach, O. *et al.* Hydrological and ecological changes in western Europe between 3200 and 2000 years BP derived from lipid biomarker δD values in lake Meerfelder Maar sediments. *Q. Sci. Rev.*, **172**, 44–54 <https://doi.org/10.1016/j.quascirev.2017.07.019> (2017).
4. Honeychurch, W. *Inner Asia and the Spatial Politics of Empire. Archaeology, Mobility, and Culture Contact* (Springer, New York, 2015).

5. Horvath, V. Horse Burials in Chamber 31 of the Arzhan-1 Mound (new data on cultural relations in the Eurasian steppes in the 8th – early 6th centuries BC). *tpai* **31**, 134–153; [10.14258/tpai\(2020\)3\(31\).-11](https://doi.org/10.14258/tpai(2020)3(31).-11) (2020).
6. Fernández-Giménez, M. E. *et al.* Exploring linked ecological and cultural tipping points in Mongolia. *Anthropocene*, **17**, 46–69 <https://doi.org/10.1016/J.ANCENE.2017.01.003> (2017).
7. Honeychurch, W. A. & Complexities The Archaeology of Pastoral Nomadic States. *J Archaeol Res*, **22**, 277–326 <https://doi.org/10.1007/s10814-014-9073-9> (2014).
8. Di Cosmo, N., Oppenheimer, C. & Büntgen, U. Interplay of environmental and socio-political factors in the downfall of the Eastern Türk Empire in 630 CE. *Clim. Change*, **145**, 383–395 <https://doi.org/10.1007/s10584-017-2111-0> (2017).
9. Di Cosmo, N. *et al.* Environmental Stress and Steppe Nomads: Rethinking the History of the Uyghur Empire (744–840) with Paleoclimate Data. *Journal of Interdisciplinary History*, **48**, 439–463 https://doi.org/10.1162/JINH_a_01194 (2018).
10. Dagvadorj, D., Natsagdorj, L., Dorjpurev, J. & Namkhainyam, B. Mongolia assessment report on climate change 2009 2009.
11. Taylor, W. *et al.* High altitude hunting, climate change, and pastoral resilience in eastern Eurasia. *Sci Rep*, **11**, <https://doi.org/10.1038/s41598-021-93765-w> (2021).
12. Zhang, P. *et al.* Abrupt shift to hotter and drier climate over inner East Asia beyond the tipping point. *Science (New York, N.Y.)*, **370**, 1095–1099 <https://doi.org/10.1126/science.abb3368> (2020).
13. Nandintsetseg, B. & Shinoda, M. Multi-Decadal Soil Moisture Trends in Mongolia and Their Relationships to Precipitation and Evapotranspiration. *Arid Land Research and Management*, **28**, 247–260 <https://doi.org/10.1080/15324982.2013.861882> (2014).
14. Nandintsetseg, B. *et al.* Risk and vulnerability of Mongolian grasslands under climate change. *Environ. Res. Lett*, **16**, 34035 <https://doi.org/10.1088/1748-9326/abdb5b> (2021).
15. Hessel, A. E. *et al.* Past and future drought in Mongolia. *Science advances*, **4**, e1701832 <https://doi.org/10.1126/sciadv.1701832> (2018).
16. Mijiddorj, T. N., Alexander, J. S., Samelius, G., Mishra, C. & Boldgiv, B. Traditional livelihoods under a changing climate: herder perceptions of climate change and its consequences in South Gobi, Mongolia. *Clim. Change*, **162**, 1065–1079 <https://doi.org/10.1007/s10584-020-02851-x> (2020).
17. Goulden, C. E. *et al.* Interviews of Mongolian herders and high resolution precipitation data reveal an increase in short heavy rains and thunderstorm activity in semi-arid Mongolia. *Clim. Change*, **136**, 281–295 <https://doi.org/10.1007/s10584-016-1614-4> (2016).
18. Blaauw, M. & Christen, J. A. Flexible paleoclimate age-depth models using an autoregressive gamma process. *Bayesian Anal*, **6**, 457–474 <https://doi.org/10.1214/11-BA618> (2011).
19. Biskop, S., Maussion, F., Krause, P. & Fink, M. Differences in the water-balance components of four lakes in the southern-central Tibetan Plateau. *Hydrol. Earth Syst. Sci*, **20**, 209–225 <https://doi.org/10.5194/hess-20-209-2016> (2016).

20. MacCallum, S. N. & Merchant, C. J. Surface water temperature observations of large lakes by optimal estimation. *Canadian Journal of Remote Sensing*, **38**, 25–45 <https://doi.org/10.5589/m12-010> (2012).
21. Laskar, J., Fienga, A., Gastineau, M. & Manche, H. La2010: a new orbital solution for the long-term motion of the Earth. *A&A* **532**, A89; [10.1051/0004-6361/201116836](https://doi.org/10.1051/0004-6361/201116836) (2011).
22. Peck, J. A. *et al.* Mid to Late Holocene climate change in north central Mongolia as recorded in the sediments of Lake Telmen. *Palaeogeography, Palaeoclimatology, Palaeoecology* **183**, 135–153; [10.1016/S0031-0182\(01\)00465-5](https://doi.org/10.1016/S0031-0182(01)00465-5) (2002).
23. Lehmkuhl, F., Grunert, J., Hülle, D., Batkhisig, O. & Stauch, G. Paleolakes in the Gobi region of southern Mongolia. *Quaternary Science Reviews* **179**, 1–23; [10.1016/j.quascirev.2017.10.035](https://doi.org/10.1016/j.quascirev.2017.10.035) (2018).
24. Fowell, S. J., Hansen, B. C.S., Peck, J. A., Khosbayar, P. & Ganbold, E. Mid to late Holocene climate evolution of the Lake Telmen Basin, North Central Mongolia, based on palynological data. *Quat. res.* **59**, 353–363; [10.1016/S0033-5894\(02\)00020-0](https://doi.org/10.1016/S0033-5894(02)00020-0) (2003).
25. Grunert, J., Lehmkuhl, F. & Walther, M. Paleoclimatic evolution of the Uvs Nuur basin and adjacent areas (Western Mongolia). *Quaternary International* **65-66**, 171–192; [10.1016/S1040-6182\(99\)00043-9](https://doi.org/10.1016/S1040-6182(99)00043-9) (2000).
26. Unkelbach, J., Dulamsuren, C., Klinge, M. & Behling, H. Holocene high-resolution forest-steppe and environmental dynamics in the Tarvagatai Mountains, north-central Mongolia, over the last 9570 cal yr BP. *Quaternary Science Reviews* **266**, 107076; [10.1016/j.quascirev.2021.107076](https://doi.org/10.1016/j.quascirev.2021.107076) (2021).
27. Jacoby, D'Arrigo & Davaajamts. Mongolian Tree Rings and 20th-Century Warming. *Science (New York, N.Y.)* **273**, 771–773; [10.1126/science.273.5276.771](https://doi.org/10.1126/science.273.5276.771) (1996).
28. D'Arrigo, R. *et al.* 1738 years of Mongolian temperature variability inferred from a tree-ring width chronology of Siberian pine. *Geophys. Res. Lett.* **28**, 543–546; [10.1029/2000GL011845](https://doi.org/10.1029/2000GL011845) (2001).
29. Davi, N. K. *et al.* A long-term context (931–2005 C.E.) for rapid warming over Central Asia. *Quaternary Science Reviews* **121**, 89–97; [10.1016/j.quascirev.2015.05.020](https://doi.org/10.1016/j.quascirev.2015.05.020) (2015).
30. Klinge, M. & Sauer, D. Spatial pattern of Late Glacial and Holocene climatic and environmental development in Western Mongolia - A critical review and synthesis. *Quaternary Science Reviews* **210**, 26–50; [10.1016/j.quascirev.2019.02.020](https://doi.org/10.1016/j.quascirev.2019.02.020) (2019).
31. van Geel, B. *et al.* Climate change and the expansion of the Scythian culture after 850 BC: a hypothesis. *Journal of Archaeological Science* **31**, 1735–1742; [10.1016/j.jas.2004.05.004](https://doi.org/10.1016/j.jas.2004.05.004) (2004).
32. Büntgen, U. *et al.* Cooling and societal change during the Late Antique Little Ice Age from 536 to around 660 AD. *Nature Geosci* **9**, 231–236; [10.1038/NGEO2652](https://doi.org/10.1038/NGEO2652) (2016).
33. Büntgen, U. *et al.* Prominent role of volcanism in Common Era climate variability and human history. *Dendrochronologia* **64**, 125757; [10.1016/j.dendro.2020.125757](https://doi.org/10.1016/j.dendro.2020.125757) (2020).
34. Sigl, M. *et al.* Timing and climate forcing of volcanic eruptions for the past 2,500 years. *Nature* **523**, 543–549; [10.1038/nature14565](https://doi.org/10.1038/nature14565) (2015).

35. Taylor, W. T. T. Building a scientific model for East Asian pastoral origins: A reply to Honeychurch et al. *Archaeological Research in Asia* **26**, 100286; 10.1016/j.ara.2021.100286 (2021).
36. Steinhilber, F. et al. 9,400 years of cosmic radiation and solar activity from ice cores and tree rings. *Proceedings of the National Academy of Sciences of the United States of America* **109**, 5967–5971; 10.1073/pnas.1118965109 (2012).
37. Strobel, P., Struck, J., Zech, R. & Bliedtner, M. The spatial distribution of sedimentary compounds and their environmental implications in surface sediments of Lake Khar Nuur (Mongolian Altai). *Earth Surf. Process. Landforms* **55**, 319; 10.1002/esp.5049 (2021).
38. Struck, J. et al. Leaf wax n-alkane patterns and compound-specific $\delta^{13}\text{C}$ of plants and topsoils from semi-arid and arid Mongolia. *Biogeosciences* **17**, 567–580; 10.5194/bg-17-567-2020 (2020a).
39. Struck, J. et al. Leaf Waxes and Hemicelluloses in Topsoils Reflect the $\delta^2\text{H}$ and $\delta^{18}\text{O}$ Isotopic Composition of Precipitation in Mongolia. *Front. Earth Sci.* **8**, 619; 10.3389/feart.2020.00343 (2020b).
40. Sachse, D. et al. Molecular Paleohydrology: Interpreting the Hydrogen-Isotopic Composition of Lipid Biomarkers from Photosynthesizing Organisms. *Annu. Rev. Earth Planet. Sci.* **40**, 221–249; 10.1146/annurev-earth-042711-105535 (2012).
41. Ficken, K.J., Li, B., Swain, D.L. & Eglinton, G. An n-alkane proxy for the sedimentary input of submerged/floating freshwater aquatic macrophytes. *Organic Geochemistry* **31**, 745–749; 10.1016/S0146-6380(00)00081-4 (2000).
42. Aichner, B. et al. Hydroclimate in the Pamirs Was Driven by Changes in Precipitation-Evaporation Seasonality Since the Last Glacial Period. *Geophysical Research Letters* **46**, 13972–13983; 10.1029/2019gl085202 (2019).
43. Mügler, I. et al. Effect of lake evaporation on δD values of lacustrine n-alkanes: A comparison of Nam Co (Tibetan Plateau) and Holzmaar (Germany). *Organic Geochemistry* **39**, 711–729; 10.1016/j.orggeochem.2008.02.008 (2008).
44. Wünnemann, B. et al. A 14 ka high-resolution $\delta^{18}\text{O}$ lake record reveals a paradigm shift for the process-based reconstruction of hydroclimate on the northern Tibetan Plateau. *Quaternary Science Reviews* **200**, 65–84; 10.1016/j.quascirev.2018.09.040 (2018).
45. Lan, J. et al. Late Holocene hydroclimatic variation in central Asia and its response to mid-latitude Westerlies and solar irradiance. *Quaternary Science Reviews* **238**, 106330; 10.1016/j.quascirev.2020.106330 (2020).
46. Horton, T. W., Defliese, W. F., Tripathi, A. K. & Oze, C. Evaporation induced ^{18}O and ^{13}C enrichment in lake systems: A global perspective on hydrologic balance effects. *Quaternary Science Reviews* **131**, 365–379; 10.1016/j.quascirev.2015.06.030 (2016).
47. Chen, F. et al. Westerlies Asia and monsoonal Asia: Spatiotemporal differences in climate change and possible mechanisms on decadal to sub-orbital timescales. *Earth-Science Reviews* **192**, 337–354; 10.1016/j.earscirev.2019.03.005 (2019).

48. Engels, S. & van Geel, B. The effects of changing solar activity on climate: contributions from palaeoclimatological studies. *J. Space Weather Space Clim.* **2**, A09; 10.1051/swsc/2012009 (2012).
49. Lean, J. L. Cycles and trends in solar irradiance and climate. *Wiley Interdisciplinary Reviews: Climate Change* **1**, 111–122; 10.1002/wcc.18 (2010).
50. Routson, C. C. *et al.* Mid-latitude net precipitation decreased with Arctic warming during the Holocene. *Nature* **568**, 83–87; 10.1038/s41586-019-1060-3 (2019).
51. Faust, J. C., Fabian, K., Milzer, G., Giraudeau, J. & Knies, J. Norwegian fjord sediments reveal NAO related winter temperature and precipitation changes of the past 2800 years. *Earth and Planetary Science Letters* **435**, 84–93; 10.1016/j.epsl.2015.12.003 (2016).
52. Tao, S. *et al.* Rapid loss of lakes on the Mongolian Plateau. *Proceedings of the National Academy of Sciences of the United States of America* **112**, 2281–2286; 10.1073/pnas.1411748112 (2015).
53. Lehmkuhl, F. *et al.* Holocene geomorphological processes and soil development as indicator for environmental change around Karakorum, Upper Orkhon Valley (Central Mongolia). *CATENA* **87**, 31–44; 10.1016/j.catena.2011.05.005 (2011).
54. Yao, Y. *et al.* Abrupt Freshening Since the Early Little Ice Age in Lake Sayram of Arid Central Asia Inferred From an Alkenone Isomer Proxy. *Geophys. Res. Lett.* **47**, 348; 10.1029/2020GL089257 (2020).
55. Borgerhoff Mulder, M. *et al.* Pastoralism and Wealth Inequality. *Current Anthropology* **51**, 35–48; 10.1086/648561 (2010).
56. Büntgen, U. & Di Cosmo, N. Climatic and environmental aspects of the Mongol withdrawal from Hungary in 1242 CE. *Scientific reports* **6**, 25606; 10.1038/srep25606 (2016).
57. Allard, F., Erdenebaatar, D., Olsen, S., Cavalla, A. & Maggiore, E. *Ritual horses in Bronze Age and present day Mongolia: some preliminary observations from Khanuy Valley*. L. Popova, S. Hartley, A. Smith (Eds.), *Social Orders and Social Landscapes (Proceedings of the 2005 University of Chicago Conference on Eurasian Archaeology)*, Cambridge Scholars, Newcastle (2007).
58. Lepetz, S. *et al.* Customs, rites, and sacrifices relating to a mortuary complex in Late Bronze Age Mongolia (Tsatsyn Ereg, Arkhangai). *Anthropozoologica* **54**, 151; 10.5252/anthropozoologica2019v54a15 (2019).
59. Bayarsaikhan, J. *Archaeological Research at Shurgakhiin Am Deer Stone Site in Zavkhan Province, Telmen Sum, Uguumur Bag. National Museum of Mongolia, Ulaanbaatar* (2013).
60. Allard, F. & Erdenebaatar, D. Khirigsuurs, ritual and mobility in the Bronze Age of Mongolia. *Antiquity* **79**, 547–563; 10.1017/S0003598X00114498 (2005).
61. van Geel, B. & Berglund, B. E. A causal link between a climatic deterioration around 850 cal BC and a subsequent rise in human population density in NW-Europe? *Terra Nostra*, 126–130 (2000).
62. van Geel, B., BUURMAN, J. & WATERBOLK, H. T. Archaeological and palaeoecological indications of an abrupt climate change in The Netherlands, and evidence for climatological teleconnections around 2650 BP. *J. Quaternary Sci.* **11**, 451–460; 10.1002/(SICI)1099-1417(199611/12)11:6<451::AID-JQS275>3.0.CO;2-9 (1996).

63. Jiang, L., Guli, J., Bao, A., Guo, H. & Ndayisaba, F. Vegetation dynamics and responses to climate change and human activities in Central Asia. *The Science of the total environment* **599-600**, 967–980; 10.1016/j.scitotenv.2017.05.012 (2017).
64. Rach, O. *et al.* Hydrological and ecological changes in western Europe between 3200 and 2000 years BP derived from lipid biomarker δD values in lake Meerfelder Maar sediments. *Quaternary Science Reviews* **172**, 44–54; 10.1016/j.quascirev.2017.07.019 (2017).
65. Honeychurch, W. *Inner Asia and the Spatial Politics of Empire. Archaeology, Mobility, and Culture Contact* (Springer, New York, 2015).
66. Horvath, V. Horse Burials in Chamber 31 of the Arzhan-1 Mound (new data on cultural relations in the Eurasian steppes in the 8th – early 6th centuries BC). *tpai* **31**, 134–153; 10.14258/tpai(2020)3(31).-11 (2020).
67. Fernández-Giménez, M. E. *et al.* Exploring linked ecological and cultural tipping points in Mongolia. *Anthropocene*, **17**, 46-69; 10.1016/J.ANCENE.2017.01.003 (2017).
68. Honeychurch, W. Alternative Complexities: The Archaeology of Pastoral Nomadic States. *J Archaeol Res* **22**, 277–326; 10.1007/s10814-014-9073-9 (2014).
69. Di Cosmo, N., Oppenheimer, C. & Büntgen, U. Interplay of environmental and socio-political factors in the downfall of the Eastern Türk Empire in 630 CE. *Climatic Change* **145**, 383–395; 10.1007/s10584-017-2111-0 (2017).
70. Di Cosmo, N. *et al.* Environmental Stress and Steppe Nomads: Rethinking the History of the Uyghur Empire (744–840) with Paleoclimate Data. *Journal of Interdisciplinary History* **48**, 439–463; 10.1162/JINH_a_01194 (2018).
71. Dagvadorj, D., Natsagdorj, L., Dorjpurev, J. & Namkhainyam, B. Mongolia assessment report on climate change 2009, 2009.
72. Taylor, W. *et al.* High altitude hunting, climate change, and pastoral resilience in eastern Eurasia. *Sci Rep* **11**; 10.1038/s41598-021-93765-w (2021).
73. Zhang, P. *et al.* Abrupt shift to hotter and drier climate over inner East Asia beyond the tipping point. *Science (New York, N.Y.)* **370**, 1095–1099; 10.1126/science.abb3368 (2020).
74. Nandintsetseg, B. & Shinoda, M. Multi-Decadal Soil Moisture Trends in Mongolia and Their Relationships to Precipitation and Evapotranspiration. *Arid Land Research and Management* **28**, 247–260; 10.1080/15324982.2013.861882 (2014).
75. Nandintsetseg, B. *et al.* Risk and vulnerability of Mongolian grasslands under climate change. *Environ. Res. Lett.* **16**, 34035; 10.1088/1748-9326/abdb5b (2021).
76. Hessel, A. E. *et al.* Past and future drought in Mongolia. *Science advances* **4**, e1701832; 10.1126/sciadv.1701832 (2018).
77. Mijiddorj, T. N., Alexander, J. S., Samelius, G., Mishra, C. & Boldgiv, B. Traditional livelihoods under a changing climate: herder perceptions of climate change and its consequences in South Gobi, Mongolia. *Climatic Change* **162**, 1065–1079; 10.1007/s10584-020-02851-x (2020).

78. Goulden, C. E. *et al.* Interviews of Mongolian herders and high resolution precipitation data reveal an increase in short heavy rains and thunderstorm activity in semi-arid Mongolia. *Climatic Change* **136**, 281–295; 10.1007/s10584-016-1614-4 (2016).
79. Blaauw, M. & Christen, J. A. Flexible paleoclimate age-depth models using an autoregressive gamma process. *Bayesian Anal.* **6**, 457–474; 10.1214/11-BA618 (2011).
80. Biskop, S., Maussion, F., Krause, P. & Fink, M. Differences in the water-balance components of four lakes in the southern-central Tibetan Plateau. *Hydrol. Earth Syst. Sci.* **20**, 209–225; 10.5194/hess-20-209-2016 (2016).
81. MacCallum, S. N. & Merchant, C. J. Surface water temperature observations of large lakes by optimal estimation. *Canadian Journal of Remote Sensing* **38**, 25–45; 10.5589/m12-010 (2012).
82. Laskar, J., Fienga, A., Gastineau, M. & Manche, H. La2010: a new orbital solution for the long-term motion of the Earth. *A&A* **532**, A89; 10.1051/0004-6361/201116836 (2011).

Figures

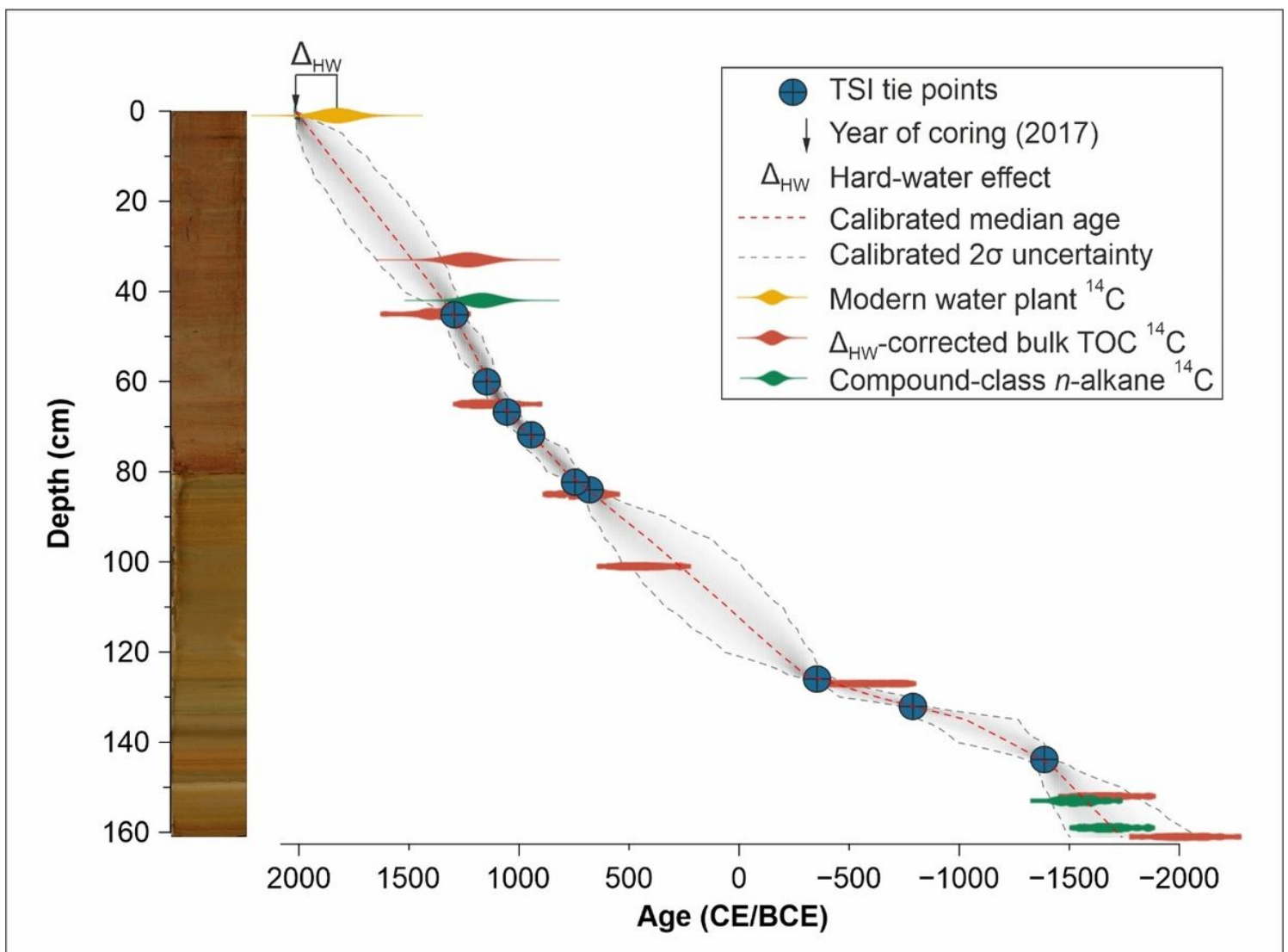


Figure 1

Photo of the sediment core from Lake Telmen, taken after oxidation, and age-depth model. The age-depth model is based on tie-points (blue dots) with the total solar irradiance (TSI)₃₆ (Supplementary Fig. 3). The ¹⁴C ages are plotted for comparison – The modern hard-water effect (Δ HW) is the difference between the year of coring in 2017 and the ¹⁴C age of a modern water plant (yellow). Δ HW-corrected bulk TOC ¹⁴C ages and compound-class n-alkane ¹⁴C ages are shown in red and green, respectively (Supplementary Tab. 1).

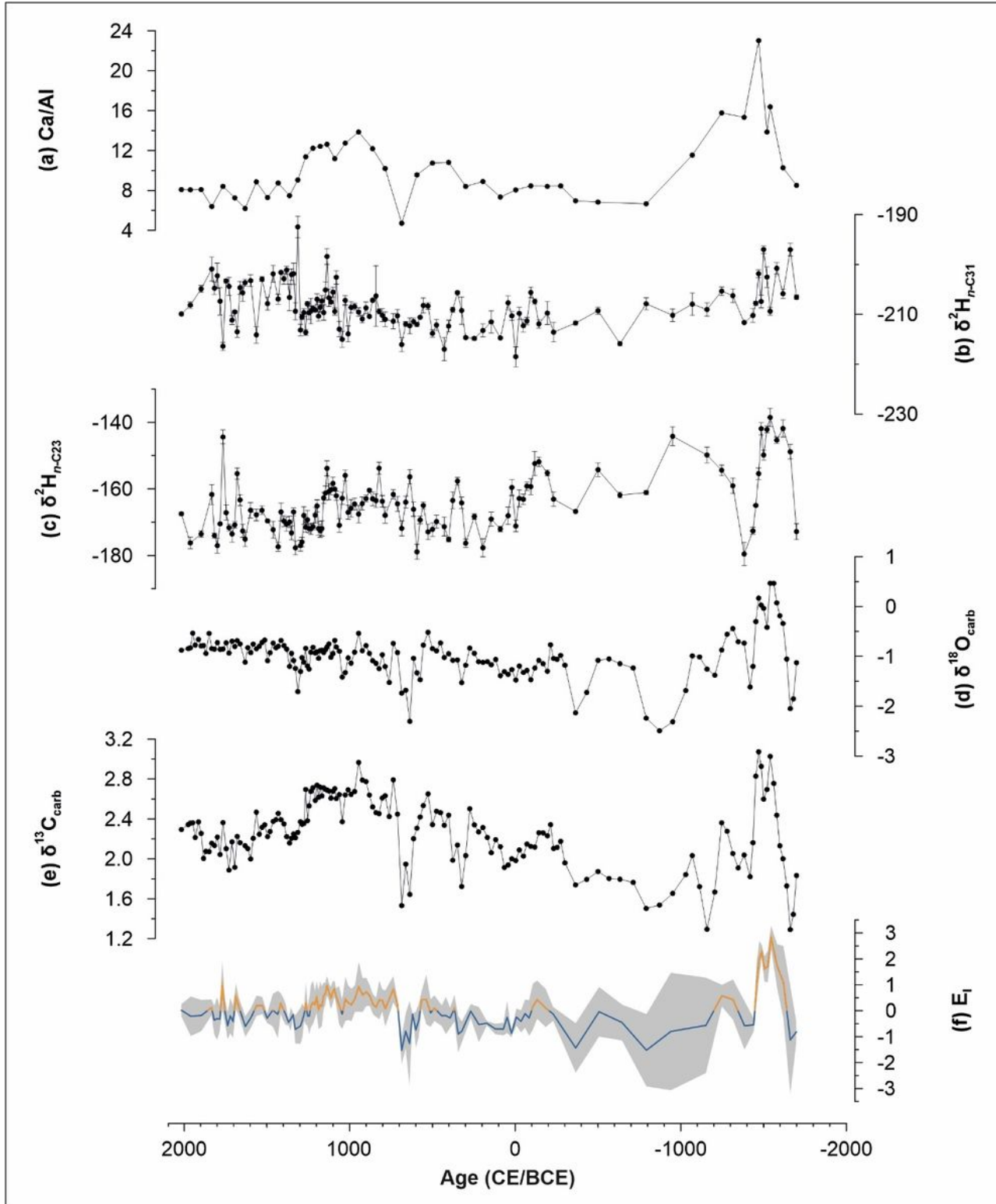


Figure 2

Geochemical and isotope records for the sediment core from Lake Telmen. (a) The Ca/Al ratio [-], (b) compound-specific $\delta^{2}\text{Hn-C31}$ [‰ vs. VSMOW], (c) compound-specific $\delta^{2}\text{Hn-C23}$ [‰ vs. VSMOW], (d) bulk carbonate $\delta^{18}\text{O}$ [‰ vs. VPDB], (e) bulk carbonate $\delta^{13}\text{C}$ [‰ vs. VPDB], and (f) evaporation index (EI) [-], yellow = dry, blue = humid, gray-shaded area = standard deviation.

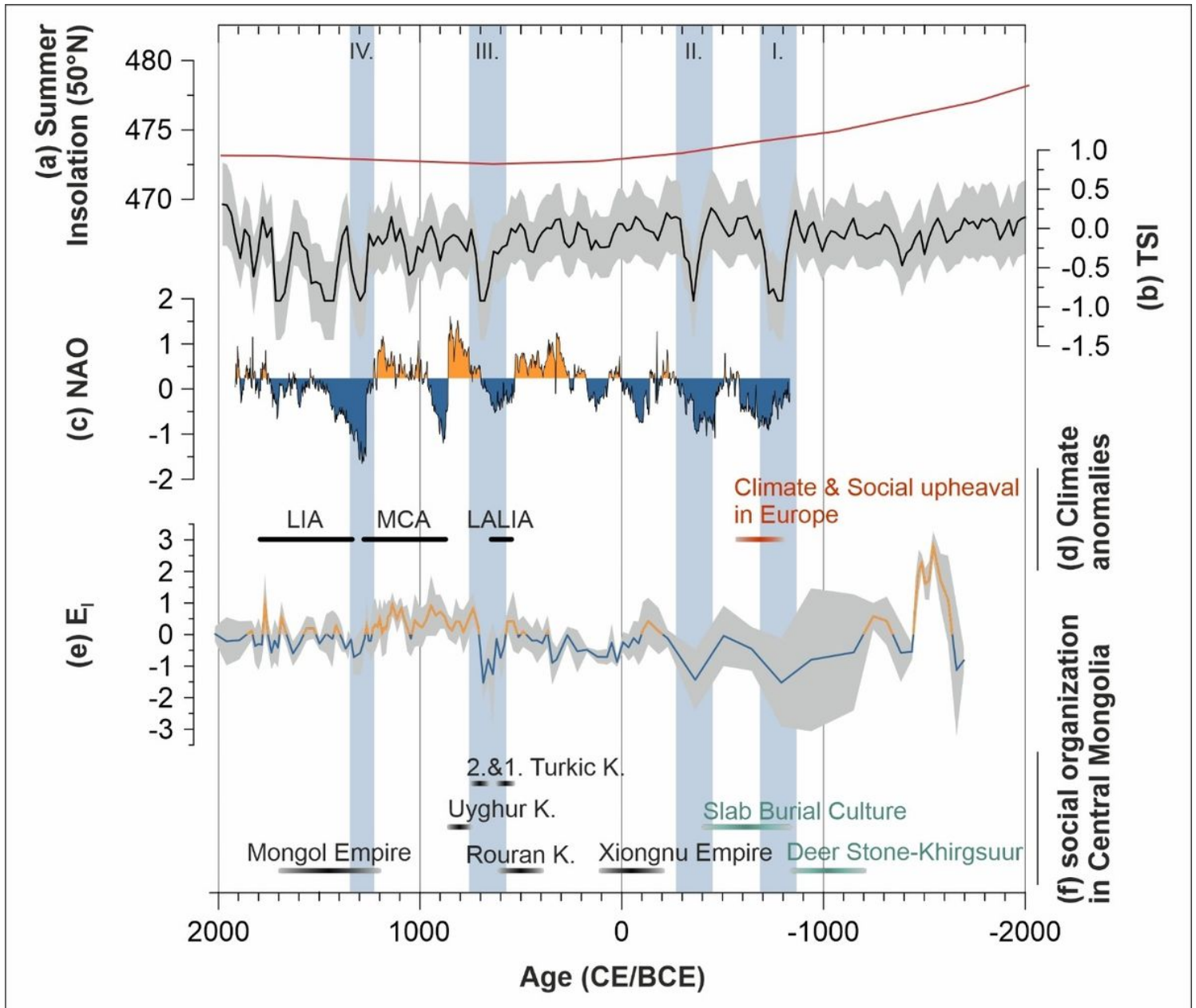


Figure 3

Late Holocene hydrological changes at Lake Telmen. (a) 50°N summer insolation [Wm⁻²]⁸², (b) total solar irradiance [Wm⁻²], gray-shaded area = 1σ uncertainty³⁶, (c) North Atlantic Oscillation (NAO) index⁵¹ [-], (d) climate anomalies during the Late Holocene: Late Antique Little Ice Age (LALIA), Medieval Climate Anomaly (MCA), and Little Ice Age (LIA) after Büntgen et al.³² and the period of social upheaval in Europe^{61,64} (e) evaporation index (EI) [-], gray-shaded area = standard deviation, (f) social organization

and duration of important Mongolian steppe cultures: Deer Stone-Khirg-suur complex (DSK), Slab Burial Culture⁶⁵, the Xiongnu^{10,68}, the Rouran Khaganate¹⁰, the first and second Turkic Khaganate^{10,69}, the Uyghur Khaganate⁷⁰ and the Mongol Empire^{10,13}. Vertical blue bars indicate distinct solar minima at ~800 BCE, 400 BCE, as well as ~700 CE and ~1300 CE.

Supplementary Files

This is a list of supplementary files associated with this preprint. Click to download.

- [20210922Strucketal.SI.pdf](#)